Observation of large frequency shifts of the electron paramagnetic resonance of ^{87}Rb atoms due to collisions with cell walls coated with RbH salt

Emily Ulanski and Zhen Wu
Department of Physics, Rutgers University, Newark, New Jersey 07102, USA
(Received 8 April 2013; published 30 May 2014)

We report an observation of large frequency shifts on the order of several hundred Hz of the electron paramagnetic resonance (EPR) of the gas phase alkali-metal atoms (^{87}Rb) in a millimeter-sized cell coated with RbH salt. We provide convincing evidence that the observed EPR frequency shift is due to collisions with RbH-coated cell walls. The RbH coating is nuclear spin polarized by spin exchange with optically pumped ^{87}Rb vapor, and the observed frequency shift is caused by the Fermi contact interaction between the s electron of the adsorbed ^{87}Rb atom and the polarized nucleus on the salt surface. From the measured EPR frequency shift we calculated the ensemble-averaged phase shift $\delta\phi_s$ experienced by the spin polarized ^{87}Rb atoms while adsorbed on the surface. Under our experimental conditions, we found the average phase shift $\delta\phi_s \sim 70$ mrad.

DOI: 10.1103/PhysRevA.89.053431 PACS number(s): 33.35.+r, 34.35.+a, 32.60.+i, 32.70.Jz

Magnetic resonances are widely used in physics. In atomic physics, for example, they are used in precision measurements of magnetic moments [1,2], magnetometry [3], test of local Lorentz invariance [4], studies of quadrupolar wall interactions [5–11], searches for permanent electric dipole moments in atoms [12,13], and many other experiments. Therefore it is important to understand the mechanisms that can cause a shift in the magnetic resonance frequency. For example, collisions between polarized alkali-metal atoms and noble gas atoms in a gaseous mixture cause a shift both in the frequency of the electron paramagnetic resonance (EPR) of alkali-metal atoms and in the frequency of the nuclear magnetic resonance (NMR) of noble gas atoms [14–17]. The frequency shift is due to the Fermi contact interaction between the s electron of the alkali-metal atom and the nucleus of the noble gas atom during the collision. The NMR frequency can also be shifted by collisions with cell walls, which has so far been observed only for spin polarized noble gas atoms that possess a quadrupole moment such as ^{131}Xe, ^{201}Hg, and ^{83}Kr [5–11]. The observed shift is due to the quadrupole interaction between the nucleus of the adsorbed noble gas atom and the electric field gradient on the surface.

In this paper we report an observation of a shift in the EPR frequency of spin polarized gas phase alkali-metal atoms (^{87}Rb) in a cell coated with RbH salt. We provide convincing evidence that the observed EPR frequency shift is due to collisions with RbH-coated cell walls. The surface of the RbH salt is nuclear spin polarized by spin exchange with optically pumped ^{87}Rb vapor in the same fashion that the surface of the CsH salt is polarized by spin exchange with optically pumped Cs vapor [18,19]. The observed EPR frequency shift is of the order of several hundred hertz for a millimeter-sized cell, and is due to the Fermi contact interaction between the s electron of the adsorbed ^{87}Rb atom and the polarized nucleus on the salt surface. The possibility that the observed frequency shift might be due to the F centers in RbH can be reasonably ruled out because, even though the salt-coated cell, after being used for about a year, did show very slight darkening, implying the formation of F centers in the coating, the frequency shift did not noticeably change.

Our observation opens up the possibility of studying surface NMR using gas phase EPR. The measured EPR frequency shifts allowed us to deduce the ensemble average of the phase shift $\delta\phi_s$ experienced by the polarized gas phase Rb atoms during each wall collision. This phase shift is proportional to the surface nuclear polarization. Furthermore, since the frequency shift due to wall collisions, unlike that due to gas phase collisions, increases with decreasing cell size, our observation implies that collisions with cell walls may cause a systematic error, the magnitude of which has yet to be determined, in the magnetic resonance frequency in high precision miniature atomic magnetometry.

The Fermi contact interaction Hamiltonian is

$$H = \alpha \boldsymbol{S} \cdot \boldsymbol{K}, \tag{1}$$

where $\boldsymbol{S}$ is the spin (in units of $\hbar$) of the s electron of the adsorbed ^{87}Rb atom, $\boldsymbol{K}$ is the nuclear spin (in units of $\hbar$) of the ion (Rb^+ or H^+) on the RbH surface, and α is the coupling constant with the dimension of energy. The Fermi contact interaction of the s electron of the adsorbed ^{87}Rb atom with the nucleus of Rb^+ is much larger than that with the nucleus (proton) of H^+ on the RbH surface [20,21]. The experimental evidence for this was provided by the observation that on the CsH surface the NMR signal of the alkali (Cs) nucleus is much larger than that of the proton [19]. Therefore, the frequency shift observed in our experiment is probably contributed mainly by the Rb^+ nuclei on the walls.

A simple semiclassical way to understand this frequency shift is the following. The coupling constant α depends on the distance between the adsorbed ^{87}Rb atom and the Rb^+ nucleus on the surface, and therefore varies while the ^{87}Rb atom bounces around on the RbH surface. As a first-order approximation we will assume α to be constant, equal to its average value. The Hamiltonian $\alpha \boldsymbol{S} \cdot \boldsymbol{K}$ can be written as $-\boldsymbol{\mu}_S \cdot \alpha \boldsymbol{K}/g_S\mu_B$, where $\boldsymbol{\mu}_S = -g_S\mu_B\boldsymbol{S}$ is the magnetic moment of the s electron, μ_B being the Bohr magneton and g_S the electron g factor. Thus the Fermi contact interaction can be regarded as a precession around a magnetic field $\alpha\langle K_z\rangle/g_S\mu_B$. The average phase shift due to the precession around this field during the average dwell time τ_s for the adsorbed Rb atom in the $I + 1/2$ level is

$$\delta\phi_s = \frac{2\pi(\alpha/h)\langle K_z\rangle\tau_s}{2I+1}, \tag{2}$$

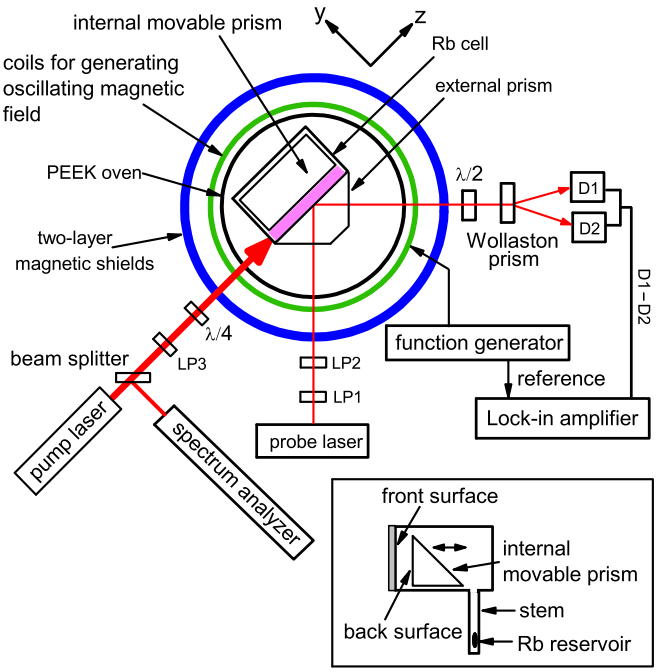

FIG. 1. (Color online) Experimental setup (top view). The pair of Glan-Thompson linear polarizers LP1 and LP2 is used as an adjustable attenuator and also ensures that the probe beam is s-polarized. The linear polarizer LP3 and the $\lambda/4$ wave plate are used to produce a σ^+ or σ^-pump beam. The pink strip is the top view of the slab-shaped cell. An external fused quartz prism is attached to the outer surface of the front window of the cell using index matching silicone fluid. Not shown in the figure are the HeNe laser and lens assembly used to measure the cell length by retroreflection. Inset: A Rb cell of adjustable length (side view).

where $I = 3/2$ is the nuclear spin of the adsorbed ^{87}Rb atom. The coherently accumulated phases during repeated wall collisions give rise to an EPR frequency shift of the ^{87}Rb atom.

Experimentally we measured the EPR frequencies $\omega^{(+)}$ and $\omega^{(-)}$ of the gas phase ^{87}Rb atoms corresponding to σ^+ and σ^- pumping beams of the same intensity for a number of different cell lengths L. Experiments were performed in cylindrical Pyrex glass cells with an inner diameter of 23 mm. The cell contained isotopically enriched rubidium (98.3 at.% ^{87}Rb) and nitrogen buffer gas of 6.0×10^{-3} amagat. A movable glass prism inside the cell acted as the adjustable back wall of the cell (see inset of Fig. 1). The effective cell length (L) is the distance between the inner surface of the front window of the cell and the front surface of the internal movable prism. In the present experiment L was varied between 1.3 and 2.5 mm by tapping the stage on which the cell was fastened. A HeNe laser was used to measure the cell thickness by retroreflection with an accuracy of 20 μm [22]. The inner surfaces of the cell and those of the prism inside the cell were coated with RbH salt following the procedure in Ref. [18]. Natural abundance rubidium was used in forming the salt. The thickness of the RbH coating is estimated to be about 2.5 μm [18]. The glass cell was held inside an oven made of PEEK, and was heated by blowing hot air into the oven. The temperature of the stem of the cell, where the ^{87}Rb metal was, was 94 °C whereas that of the cell body was 110.8 °C so as to prevent Rb condensation on the coatings. Great care was taken to prevent the RbH surfaces from being contaminated by Rb films in the manufacturing of the cells. Both the cell and the oven were placed inside two concentric cylindrical μ-metal shields (Fig. 1). Both ends of the cylindrical shields were also covered with μ-metal caps. A set of Helmholtz coils inside the shields provided a homogeneous magnetic field of about 0.1 G along the $+z$ direction. The holding field was not actively locked, but monitored with a magnetometer of a similar design as the one used in Ref. [9], and was found to be stable to better than 40 μG. The ^{87}Rb atoms in the vapor were optically pumped using a σ^+ or σ^- polarized beam from a diode laser. The pump beam propagated along the $+z$ direction, and was expanded sufficiently so that it illuminated the entire cell uniformly. Its intensity was $\sim$5 mW/cm^2 and its frequency was tuned slightly ($\sim$600 MHz) to the high frequency side of the transitions $F = 1 \rightarrow F' = 1,2$ of the ^{87}Rb D_1 line (794.8 nm) in order to pump the vapor more uniformly. Therefore only repopulation pumping contributed to the vapor polarization, which was estimated to be $\langle S_z \rangle \sim 0.03$. We measured the Zeeman transition frequency (Larmor frequency) of the $F = 2$ level, which was subject to light shift (Stark effect) due to the pump beam [23]. The reasons for choosing this inefficient way to polarize the vapor, i.e., pumping only from the $F = 1$ level, are (1) to guarantee that the light shift is opposite to the helicity of the pumping light [23] and therefore we can be sure that the observed frequency shift that has the same sign as the helicity of the pumping light is not due to light shift; and (2) to make the light shift of the Zeeman transitions in the $F = 2$ level insensitive to the frequency drift of the pump beam [23]. A Fabry-Perot spectrum analyzer was used to monitor the frequency of the pump beam so that its frequency did not drift by more than 40 MHz. The ^{87}Rb atoms in the vapor were probed in the vicinity ($\sim 10^{-4}$ cm) of the front surface of the cell using a weak s-polarized evanescent beam from a second diode laser tuned to the transitions $F = 2 \rightarrow F' = 1,2$ of the ^{87}Rb D_1 line. The probe beam size was about 2.0 mm in diameter. The linewidth of both the pump and probe beams was 40 MHz. An oscillating magnetic field $2B_1 \cos(\omega t)$ was applied along the x axis. The rotation of the polarization plane (Faraday rotation) of the probe beam depended on the polarization in the $F = 2$ level, which in turn depended on the frequency ω of the oscillating magnetic field. The Faraday rotation was measured as an imbalance in the outputs of two identical silicon photodiodes, which had been balanced for unpolarized ^{87}Rb vapor using the combination of a half-wave plate and a Wollaston prism. In order to use a phase sensitive detection technique we modulated the Faraday rotation by modulating the amplitude of the oscillating magnetic field at 200 Hz, a frequency that was chosen to maximize the signal-to-noise ratio. The modulated outputs of the two detectors were fed into a lock-in amplifier, the output of which was proportional to the modulation amplitude of the Faraday rotation, and yielded a magnetic resonance curve when the frequency ω of the oscillating magnetic field scanned across the ^{87}Rb Zeeman resonance. Because the RbH-coated walls are strongly relaxing compared with walls coated with, for example, octadecyltrichlorosilane (OTS)—a common antirelaxation coating—the signal-to-noise ratio of the EPR signal in RbH-coated cells is much worse than that

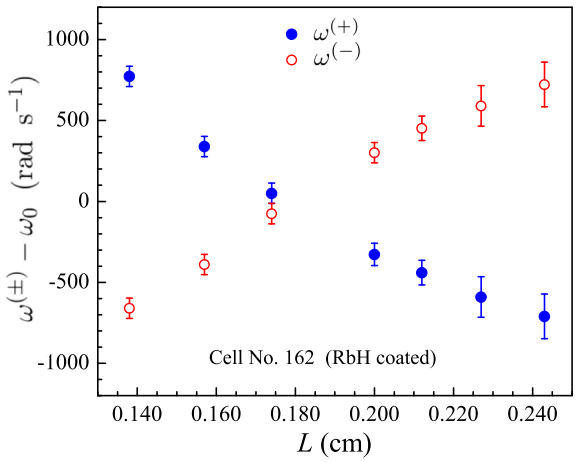

FIG. 2. (Color online) The dependence of the measured EPR frequency shifts $\omega^{(-)} - \omega_0$ (open red circles) and $\omega^{(+)} - \omega_0$ (filled blue circles) on the cell length L. The experimental conditions for the data in Figs. 2 and 3 are the same and are described in the text.

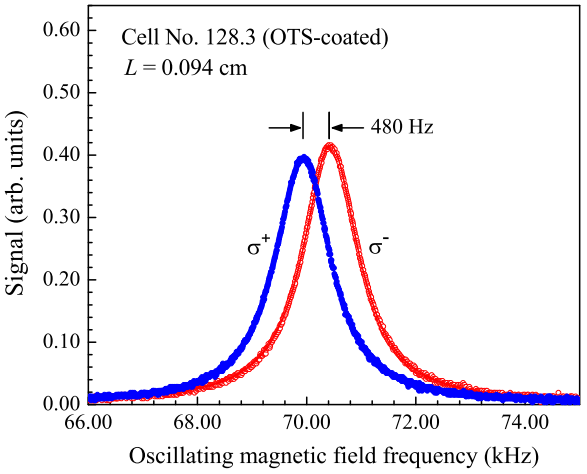

FIG. 3. (Color online) The measured EPR curves in an OTS-coated cell under the same experimental conditions as in Fig. 2. The OTS-coated cell has the same N_2 density as the RbH-coated cell. The blue curve corresponds to σ^+ pumping and therefore $\omega^{(+)}$. The red curve corresponds to σ^- pumping and therefore $\omega^{(-)}$. The shift between these two curves is equal to twice the light shift.

in OTS-coated cells. However, reproducible peak frequencies (within experimental errors) of the EPR curves were obtained for measurements made under the same experimental conditions. This reproducibility provides a basis for a quantitative study of the EPR frequency shift in RbH-coated cells.

The measured EPR frequency is given by

$$\omega^{(\pm)} = \omega_0 \pm \delta\omega_{\text{light}} \pm \delta\omega_s, \tag{3}$$

where ω_0 is the EPR frequency of the ^{87}Rb atom due to the holding field [24], $\pm\delta\omega_{\text{light}}$ is the light shift due to $\sigma^{\pm}$ pump beam, and $\pm\delta\omega_s$ is the frequency shift due to wall collisions for $\sigma^{\pm}$ pumping. As mentioned before, since we pump the ^{87}Rb atoms from the $F = 1$ level and probe the Zeeman resonances of the $F = 2$ level, we have $\delta\omega_{\text{light}} < 0$ [23]. That is, the Stark effect causes a negative frequency shift for σ^+ pumping and a positive one for σ^- pumping. The opposite is true for the frequency shift due to collisions with polarized walls.

Shown in Fig. 2 is the dependence of the measured EPR frequency shifts $\omega^{(\pm)} - \omega_0$ on the cell length L. The values of ω_0 as obtained from $\omega_0 = (\omega^{(+)} + \omega^{(-)})/2$ for each L fluctuate around its mean, which is used in Fig. 2, by no more than $2\pi \times 24$ rad s^{-1}. We note that $\omega^{(\pm)} - \omega_0$ is expected to approach a constant $\pm\delta\omega_{\text{light}} = \mp 2\pi \times 240$ rad s^{-1} [see discussions below Eq. (14)] for large L, when the frequency shift due to wall collisions becomes negligible. One sees that for small L the frequency shift due to wall collisions outweighs the light shift and $\omega^{(+)} > \omega^{(-)}$, whereas for large L the opposite is true and we have $\omega^{(-)} > \omega^{(+)}$, in agreement with the semiclassical theory of light shift [23]. The observation that the difference $\omega^{(-)} - \omega^{(+)}$ in the measured EPR frequencies changes sign from negative to positive as the cell length L increases proves that the observed frequency shift is not owing to gas phase processes but to collisions with cell walls.

Further evidence is provided by the data shown in Fig. 3, which displays a pair of ^{87}Rb magnetic resonance curves taken under the same experimental conditions but in an OTS-coated cell. One sees the dramatic difference between the data taken in RbH- and OTS-coated cells. In RbH-coated cells, under our experimental conditions, we have $\omega^{(+)} > \omega^{(-)}$ for cell length $\leqslant 0.18$ cm, whereas in the OTS-coated cell, which has a cell length of 0.094 cm, we still have $\omega^{(+)} < \omega^{(-)}$, that is, the light shift still dominates. In fact, in OTS-coated cells, under any of our experimental conditions, we have not observed $\omega^{(+)} > \omega^{(-)}$, implying that the EPR frequency shift due to collisions with OTS-coated walls is not detectable in the present experiment. The difference between the data taken in RbH-coated and OTS-coated cells provides convincing evidence that the observed frequency shift is due to collisions with RbH-coated walls.

The measured EPR frequency shifts allowed us to calculate the average phase shift $\delta\phi_s$ experienced by a polarized ^{87}Rb atom while adsorbed on the wall. The EPR frequencies in the presence of wall interactions are given by the imaginary part of the eigenvalues of the following diffusion equation [11,25,26]:

$$\left(D\frac{d^2}{dy^2} - i\omega_0 \mp i\delta\omega_{\text{light}} + \alpha_n\right)\psi_n(y) = 0, \tag{4}$$

where α_n is the eigenvalue corresponding to the nth longitudinal mode $\psi_n(y)$, the cell axis being the y axis. We only need to consider the longitudinal modes because the diameter of the cell is more than one order of magnitude larger than the cell length. The boundary conditions for $\psi_n(y)$ at the front ($y = -L/2$) and back ($y = L/2$) surfaces are [25]

$$0 = \pm\frac{\partial}{\partial y}\psi_n(y) + \mu\psi_n(y) + \eta\frac{\partial^2}{\partial y^2}\psi_n(y)\Big|_{y=\pm L/2}, \tag{5}$$

with [27]

$$\mu = \frac{3(\xi_s \pm i\delta\phi_s)}{4\lambda} \quad \text{and} \quad \eta = \frac{\tau_s\bar{v}}{4}, \tag{6}$$

where ξ_s is the average relaxation probability for a polarized ^{87}Rb atom during the average dwell time τ_s on the cell wall, $\lambda = 3.0 \times 10^{-3}$ cm is the mean free path of ^{87}Rb atoms in the N_2 gas, and $\bar{v} = \sqrt{8kT/\pi m} = 3.0 \times 10^4$ cm/s is the mean

speed of ^{87}Rb atoms. The $\pm$ sign in front of $\delta\phi_s$ refers to $\sigma^{\pm}$ pumping.

In order to estimate the relative magnitude of the three terms on the right-hand side of the boundary condition (5), which, in dimensionless quantities, are 1, μL, and η/L, we need to estimate the magnitude of some of the parameters, such as ξ_s and τ_s. The magnitude of ξ_s can be deduced from the linewidth of the EPR curves, which in the present experiment is contributed mostly by the rf broadening. For $L = 0.15$ cm, the broadening due to wall relaxation is 1.6 kHz, from which one obtains the relaxation rate due to wall collisions, $2\pi \times 1.6\ \text{kHz} = 1.0 \times 10^4\ \text{s}^{-1}$. In order to make an estimate of ξ_s we need to know the rate of wall collisions for ^{87}Rb atoms. We note that the wall collision rate of a ^{87}Rb atom is purely a gas kinetic quantity, independent of its spin orientation. It can be derived from gas kinetic theory as follows. The total number of collisions per second of ^{87}Rb atoms on both the front and back surfaces of area A is given by $An\bar{v}/2$, which can be written as $N\bar{v}/2L$, where n and N are, respectively, the number density and the total number of ^{87}Rb atoms in the cell. Thus the rate of a single ^{87}Rb atom hitting the front or back surface is $\bar{v}/2L$. For a cell thickness of 1.5 mm, the wall collision rate is $\bar{v}/2L = 1.0 \times 10^5\ \text{s}^{-1}$. Therefore the average relaxation probability for a polarized Rb atom during a wall collision is $\xi_s = 1.0 \times 10^4\ \text{s}^{-1}/10^5\ \text{s}^{-1} = 0.1$. This value of ξ_s seems quite reasonable if we compare it with $\xi_s = 1.3 \times 10^{-3}$ obtained in an OTS-coated cell [28], and also note that the linewidth due to wall collisions in an OTS-coated cell of 0.15 cm thickness is 20 Hz [29]. Even though τ_s for Rb atoms on the RbH surface has not been reported to our knowledge, it is almost certain that the dwell time τ_s for a Rb atom on the rigid RbH salt surface is much shorter than the dwell time τ_s for a Rb atom on porous materials such as OTS and paraffin, where τ_s is found to be $\sim 10^{-6}$ s [30,31]. Therefore $\eta/L \ll 1$ on the RbH surface. Since $\mu L \sim 5$, the second derivative term in the boundary condition (5) is insignificant in the present experiment, and will be omitted. The boundary condition (5) then becomes

$$0 = \pm\frac{\partial}{\partial y}\psi_n(y) + \mu\psi_n(y)\Big|_{y=\pm L/2}. \tag{7}$$

The boundary conditions (7) were used in previous studies of surface interactions of spin polarized atoms [11,26], the difference being that μ is a real number in Ref. [26] and an operator in Ref. [11].

Because Eq. (4) and its boundary condition (7) have parity symmetry, its solutions are also eigenfunctions of parity, and proportional to either $\cos(k_n y)$ or $\sin(k_n y)$. Since the pumping beam is approximately uniform throughout the cell, the contributions from all the modes except the lowest one are negligibly small, and we will therefore only consider the lowest mode, which is proportional to $\cos(k_0 y)$ and corresponds to eigenvalue $\alpha_0 = i\omega_0 + i\delta\omega_{\text{light}} + Dk_0^2$ for σ^+ pumping. Substituting $\cos(k_0 y)$ into the boundary condition (7), we find the wave number $k_0 = 2u_0/L$, u_0 being dimensionless, to be the solution of the following equation:

$$u_0 \tan(u_0) = \frac{L\mu}{2}, \quad \text{with} \quad 0 < \text{Re}\, u_0 < \pi/2, \tag{8}$$

TABLE I. EPR frequency shifts $\delta\omega_s/2\pi$ due to wall collisions.

Cell length L (cm)	0.138	0.157	0.174	0.200	0.212	0.227	0.243
$\delta\omega_s/2\pi$ (Hz)	354	298	250	190	169	146	126

or

$$u_0 \tan(u_0) = \frac{3L\xi_s}{8\lambda} + i\frac{3L\delta\phi_s}{8\lambda}. \tag{9}$$

We write $u_0 = u_0' + iu_0''$. The EPR frequency shift due to wall collisions is given by

$$\delta\omega_s = \text{Im}\, Dk_0^2, \tag{10}$$

which can be written as

$$\delta\omega_s = \frac{8D}{L^2}u_0'u_0''. \tag{11}$$

The boundary condition, Eq. (9), can be written in terms of real and imaginary parts as

$$\frac{u_0' \tan u_0' \,\text{sech}^2 u_0'' - u_0'' \tanh u_0'' \sec^2 u_0'}{1 + \tan^2 u_0' \tanh^2 u_0''} = \frac{3L\xi_s}{8\lambda} \tag{12}$$

and

$$\frac{u_0'' \tan u_0' \,\text{sech}^2 u_0'' + u_0' \tanh u_0'' \sec^2 u_0'}{1 + \tan^2 u_0' \tanh^2 u_0''} = \frac{3L\delta\phi_s}{8\lambda}. \tag{13}$$

The frequency shift $\delta\omega_s$ due to wall collisions is deduced from the measured EPR frequencies as follows. Equation (3) can be written as

$$\delta\omega_s = \frac{-\Delta - 2\delta\omega_{\text{light}}}{2}, \tag{14}$$

where $\Delta = \omega^{(-)} - \omega^{(+)}$. The light shift $\delta\omega_{\text{light}}$ is obtained by measuring $\omega^{(-)}$ and $\omega^{(+)}$ in an OTS-coated cell, in which the shift due to wall collisions is negligible as mentioned in the above (Fig. 3). Thus we have $\delta\omega_{\text{light}} = -\Delta/2 = -2\pi \times 240\ \text{rad s}^{-1}$. The frequency shift due to wall collisions can be computed from Eq. (14) for each value of L. For example, for $L = 0.138$ cm, we found from the measured EPR frequencies $\omega^{(-)}$ and $\omega^{(+)}$ that $\Delta = -2\pi \times 228\ \text{rad s}^{-1}$ (see Fig. 2). Therefore $\delta\omega_s = (-\Delta - 2\delta\omega_{\text{light}})/2 = 2\pi \times 354\ \text{rad s}^{-1}$ or 354 Hz. Frequency shifts due to wall collisions computed this way for all the values of L are listed in Table I.

Thus, for each L, we can numerically solve Eqs. (11) and (12) for u_0' and u_0'', from which we obtain $\delta\phi_s$ from Eq. (13). We plot in Fig. 4 the numerically calculated $\delta\phi_s$ for each L. The computed values of $\delta\phi_s$ increase with L. This is because the wall relaxation rate increases with decreasing L, and therefore the ^{87}Rb vapor and consequently the surface polarization, as well as $\delta\phi_s$, decreases with decreasing L. This is consistent with the experimental observation that the Faraday rotation signal, which is proportional to the Rb vapor polarization, decreases with decreasing L. One also sees that the rate of increase of $\delta\phi_s$ with L seems to decrease as L increases. Physically this is probably due to the following reason. When L increases, the contribution to the total relaxation rate from wall interactions decreases, and the ^{87}Rb vapor polarization and consequently the wall polarization, as well as $\delta\phi_s$, becomes less dependent on L.

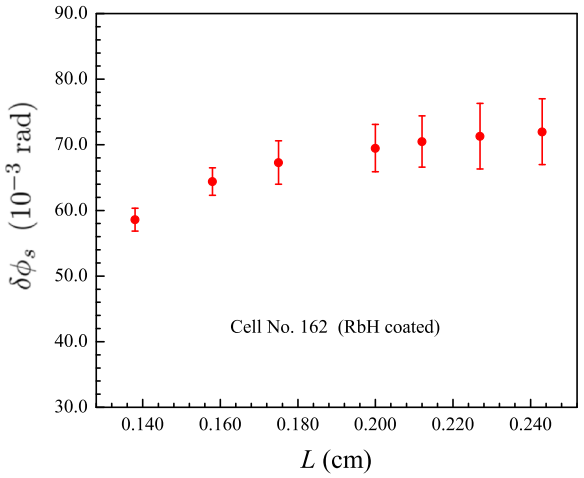

FIG. 4. (Color online) The dependence of the numerically calculated average phase shift $\delta\phi_s$ on the cell length L.

The observed EPR frequency shift is found to increase with the Rb vapor density and with the power of the pump laser. This can be understood by noting that the EPR frequency shift due to wall collisions is proportional to the wall nuclear polarization, and therefore increases with the angular momentum flux into the surface, which is proportional to the Rb vapor density and the Rb vapor polarization. The latter increases with the power of the pump beam.

We note that by measuring the average surface phase shift $\delta\phi_s$ and independently measuring the dwell time τ_s, Eq. (4) yields information on $\langle K_z \rangle$, thus providing an interesting method for measuring the surface nuclear polarization using the gas phase EPR.

We thank Martin Schaden for invaluable discussions, Kiyoshi Ishikawa for information about the RbH coating procedure, Kaifeng Zhao for his computer program used in parts of the experiment, and Thad Walker for his critical comments. We also acknowledge the support from Mike Wardlaw of the ONR.

[1] F. P. Calaprice, W. Happer, D. F. Schreiber, M. M. Lowry, E. Miron, and X. Zeng, Phys. Rev. Lett. **54**, 174 (1985).
[2] M. Kitano, F. P. Calaprice, M. L. Pitt, J. Clayhold, W. Happer, M. Kadar-Kallen, M. Musolf, G. Ulm, K. Wendt, T. Chupp, J. Bonn, R. Neugart, E. Otten, and H. T. Duong, Phys. Rev. Lett. **60**, 2133 (1988).
[3] D. Budker and M. Romalis, Nat. Phys. **3**, 227 (2007).
[4] T. E. Chupp, R. J. Hoare, R. A. Loveman, E. R. Oteiza, J. M. Richardson, M. E. Wagshul, and A. K. Thompson, Phys. Rev. Lett. **63**, 1541 (1989).
[5] J. H. Simpson, Bull. Am. Phys. Soc. **23**, 394 (1978).
[6] C. H. Volk, J. G. Mark, and B. Grover, Phys. Rev. A **20**, 2381 (1979).
[7] T. M. Kwon, J. G. Mark, and C. H. Volk, Phys. Rev. A **24**, 1894 (1981).
[8] C. Cohen-Tannoudji, J. Phys. (Paris) **24**, 653 (1963).
[9] Z. Wu, W. Happer, and J. Daniels, Phys. Rev. Lett. **59**, 1480 (1987).
[10] Z. Wu, W. Happer, M. Kitano, and J. Daniels, Phys. Rev. A **42**, 2774 (1990).
[11] Z. Wu, S. Schaefer, G. D. Cates, and W. Happer, Phys. Rev. A **37**, 1161 (1988).
[12] T. G. Vold, F. J. Raab, B. Heckel, and E. N. Fortson, Phys. Rev. Lett. **52**, 2229 (1984).
[13] W. C. Griffith, M. D. Swallows, T. H. Loftus, M. V. Romalis, B. R. Heckel, and E. N. Fortson, Phys. Rev. Lett. **102**, 101601 (2009).
[14] B. C. Grover, Phys. Rev. Lett. **40**, 391 (1978).
[15] W. Happer, E. Miron, S. Schaefer, D. Schreiber, W. A. van Wijngaarden, and X. Zeng, Phys. Rev. A **29**, 3092 (1984).
[16] S. R. Schaefer, G. D. Cates, Ting-Ray Chien, D. Gonatas, W. Happer, and T. G. Walker, Phys. Rev. A **39**, 5613 (1989).
[17] N. R. Newbury, A. S. Barton, P. Bogorad, G. D. Cates, M. Gatzke, H. Mabuchi, and B. Saam, Phys. Rev. A **48**, 558 (1993).
[18] K. Ishikawa, B. Patton, Y.-Y. Jau, and W. Happer, Phys. Rev. Lett. **98**, 183004 (2007).
[19] B. Patton, Ph.D. dissertation, Princeton University, 2007.
[20] R. M. Herman, Phys. Rev. **137**, 1062 (1965).
[21] T. Walker and W. Happer, Rev. Mod. Phys. **69**, 629 (1997).
[22] P. J. Thomas, R. Mani, and N. Khalil, Rev. Sci. Instrum. **70**, 2225 (1999).
[23] B. S. Mathur, H. Tang, and W. Happer, Phys. Rev. **171**, 11 (1968); W. Happer and B. S. Mathur, *ibid.* **163**, 12 (1967).
[24] The difference between the Zeeman transition frequencies for σ^+ and σ^- pumping due to the uneven splitting of the Zeeman energy levels is 4 Hz for the field used in the present experiment, and therefore is ignored in the analysis.
[25] M. Schaden, K. Zhao, and Z. Wu, Phys. Rev. A **76**, 062502 (2007); **77**, 049903(E) (2008).
[26] F. Masnou-Seeuws and M. A. Bouchiat, J. Phys. **28**, 406 (1967).
[27] We note that the coefficients in the definitions of μ and η in Eq. (6) are different from those in Ref. [25]. The reason for this discrepancy is that the boundary conditions in Ref. [25] were derived using a simple hopping model, whereas the coefficients in Eq. (6) are chosen so that the theory agrees with the gas kinetic theory for the EPR frequency shift when $|\mu| \ll 1$.
[28] K. Zhao, M. Schaden, and Z. Wu, Phys. Rev. A **78**, 034901 (2008).
[29] K. Zhao and Z. Wu, Appl. Phys. Lett. **93**, 101101 (2008).
[30] K. F. Zhao, M. Schaden, and Z. Wu, Phys. Rev. Lett. **103**, 073201 (2009).
[31] E. Ulanski and Z. Wu, Appl. Phys. Lett. **98**, 201115 (2011).